



North Atlantic seasonal climate variability significantly modulates extreme winter Euro-Atlantic extratropical cyclone hazards

5 Amanda C. Maycock^{1,*}, Christine M. McKenna^{1,2}, Matthew D. K. Priestley³, Jacob Perez⁴, Julia F. Lockwood⁵

¹ Institute for Climate and Atmospheric Science, School of Earth and Environment, University of Leeds, Leeds, UK

² JBA Consulting, Warrington, UK

³ Department of Mathematics and Statistics, University of Exeter, Exeter, UK

10 ⁴ Centre for Doctoral Training in Fluid Dynamics, School of Computing, University of Leeds, Leeds, UK

⁵ Met Office Hadley Centre, Exeter, UK

Correspondence to: Amanda C. Maycock (a.c.maycock@leeds.ac.uk)

Abstract. North Atlantic extratropical cyclones (ETCs) cause significant financial losses in Europe, particularly in winter. Previous work has shown seasonal relationships between ETC hazards and modes of North Atlantic atmospheric variability, including the North Atlantic Oscillation (NAO; PC1) and East Atlantic Pattern (EAP; PC2). This study examines the relationship between the most extreme ETC hazards experienced at a given location in a winter season with the NAO and EAP, focusing on the winter maximum 10 metre wind gust and coastal wave swell height and the maximum daily total precipitation. We examine compound effects where PC1 or PC2 have signals in multiple hazard types at the same location. Positive PC1 exhibits coincident increases in winter maximum wind gust and wave swell hazards around most coastal regions in northern Europe. Positive PC2 exhibits coincident increases in winter maximum wind gust and daily total precipitation hazards over land areas in southern UK, Portugal and Spain, with an additional compound effect from increased wave swell near southern UK, northern France and Spain coasts. We also consider compound effects where PC1 and PC2 show coincident signals in the same hazard at a given location, potentially indicating an elevated hazard likelihood when circulation anomalies project onto both modes concurrently. PC1 and PC2 have coincident signals for wind gusts in southern Ireland, southern UK, Portugal and Scandinavian coast. For wave swell height, PC1 and PC2 have coincident signals around the Scandinavian, southern UK and Ireland and Northern Portugal coasts. This study shows that large-scale modes of seasonal North Atlantic climate variability modulate the exposure to extreme ETC hazards in many parts of Europe. The results have the potential to be combined with skilful seasonal climate forecasts of PC1 and PC2 to inform the insurance sector.

30



1 Introduction

North Atlantic extratropical cyclones (ETC) are the primary source of winter-time weather related hazards in Europe, including
35 damaging winds, heavy precipitation and marine wave swell. These hazards have caused billions of Euros of damages in
affected seasons (e.g., Moemken et al., 2024), particularly in boreal winter when the North Atlantic storm track is most active.
Seasonal climate forecasts aim to predict the risk of weather and climate hazards several months in advance, so that preparatory
action can be taken to mitigate anticipated impacts. One source of potential predictability on seasonal-to-annual timescales is
40 via the relationship of ETC hazards with large-scale modes of atmospheric variability, which can be predictable on seasonal
timescales. In particular, seasonal forecast models have shown predictive skill for the winter North Atlantic Oscillation (NAO,
e.g., Scaife et al., 2014) and the early winter East Atlantic pattern (EAP, Thornton et al., 2023), so these modes are the focus
of this study. If a mode of variability can be skilfully predicted, then information about the exposure to ETC hazards can be
deduced (e.g., Befort et al., 2019; Degenhardt et al., 2022, 2024; Lockwood et al., 2023). It is therefore of value to derive
observed relationships between ETC hazards and modes of variability, to inform the assessment of potential sources of
45 predictive skill.

Previous work has shown the pattern of winter wind gusts (e.g., Donat et al., 2010; Befort et al., 2019; Degenhardt et al., 2022,
2024; Lockwood et al., 2023) and wave swell (e.g., Bacon & Carter, 1993; Dodet et al., 2010; Izaguirre et al., 2010, 2011;
Martinez-Asensio et al., 2016; Castle et al., 2018) in northern Europe are correlated with the NAO. Furthermore, when the
50 NAO is in a positive phase there are generally wetter winter conditions in the UK and northern Europe and drier conditions in
southern Europe (Hurrell et al., 2003). A positive EAP phase is associated with an increase in cumulative winter storm severity
in the UK, which is weaker than for the NAO (Degenhardt et al., 2022), but with relatively little signal in continental Europe.
Many existing studies consider seasonal hazards and do not explicitly consider short timescale extremes, which are often linked
to considerable impacts. Furthermore, there has been less attention paid to the relationship of North Atlantic modes of
55 variability with compound hazards, where a particular region or location may experience more than one extreme hazard within
a season (e.g., heavy precipitation and strong winds; Matthews et al., 2014, Hillier et al., 2015, Martius et al., 2016). Such
compound events can increase overall damages, leading to higher insurance claims and longer timescales to restore
infrastructure following the events (Hillier et al., 2015, 2025; Bloomfield et al., 2023). Therefore, there is value in quantifying
the relationships of compound hazards with modes of variability for the purposes of understanding potential seasonal
60 predictability.

This study addresses the following questions:

- 1) How are the two leading modes of North Atlantic atmospheric variability – the NAO and East Atlantic (EA)
65 patterns – related to spatial variability in extreme ETC hazards due to wind gusts, daily precipitation rates and wave
swell?



- 2) In which regions do the NAO and EAP induce more than one hazard (compound hazards) and in which regions do the two modes have geographically overlapping hazard signals (i.e. both modes contribute to the local risk)?

The remainder of the paper is structured as follows: Section 2 describes the datasets used in the study and the analysis methods;

70 Section 3 describes the Results and Section 4 summarises our main conclusions.

2 Methods

2.1 Datasets

The analysis uses ERA5 reanalysis data based on the Integrated Forecasting System (IFS) Cycle 41r2 (Hersbach et al., 2020). Data are extracted for the entire calendar year from 1980-2020. The variables used in the analysis are 850 hPa relative vorticity
75 (variable ‘vo’), mean sea level pressure (variable ‘msl’), maximum 10 metre wind gust since previous preprocessing (variable ‘10fg’), total precipitation (variable ‘pr’), and significant height of combined wind waves and swell (variable ‘swh’). ERA5 is provided at a 0.25x0.25 degree resolution (0.5x0.5 degrees for ‘swh’ variable) and used at 1 hourly temporal frequency.

As is standard for climate models, wind gusts are post-processed in ERA5 following the approach described in ECMWF
80 (2016). Comparison with meteorological station data in Sweden indicates strong wind gusts ($> \sim 15$ m/s) are generally underestimated in ERA5 compared to point locations (Minola et al., 2020). Lodise et al. (2024; their Fig 7) compare Northern hemisphere ETC footprints for 10m wind speeds and significant wave height in ERA5 with collocated radar altimeter measurements. They find ERA5 is biased low by $\sim 5\%$ in the region of strongest 10m wind speeds on the eastern hemisphere of the cyclone relative to the translational direction, and is low biased by $\sim 5\%$ for significant wave height across much of the
85 cyclone footprint. Therefore, the wind storm hazards derived in this study are likely to be a conservative estimate. ERA5 captures daily precipitation variability across Europe with reasonable skill compared with E-OBS observation-based data (Bandhauer et al., 2021).

2.2 ETC tracking

The TRACK algorithm is used to identify and track ETCs (Hodges, 1994, 1995, 1999). TRACK identifies ETCs based on
90 maxima in the hourly 850 hPa relative vorticity field. Prior to tracking, the vorticity field is spectrally truncated to T42 resolution and filtered to remove wavenumbers less than 5, which ensures the analysis focuses on synoptic scale disturbances. Following identification of cyclonic maxima, identification points are refined using a B-spline interpolation and steepest ascent maximization. ETCs are then grouped into tracks using a nearest neighbor approach. These are then refined by the minimization of a cost function for track smoothness subject to adaptive constraints. As we are only interested in well-
95 developed and long-lived ETCs, tracks must persist for at least 48 hours and travel at least 1000 km from their origin. Due to



the focus of this study being on Europe and the North Atlantic, only tracks that are present in the region 30-75°N, 260-40°E are retained in the analysis. For each track in the study region, we identify the atmospheric and oceanic state that is attributable to the presence of the ETC based on a distance criterion. At each hourly step in the lifecycle, the hazard ‘footprint’ around the ETC is extracted using a radial distance of either 5° or 10° from the cyclone centre. A 5° radius is used for the wind gust and wave/swell height variables and a 10° radius for precipitation. This is due to the maximum winds of an ETC mainly being within 5° of the cyclone centre (Priestley and Catto, 2022), but a larger area of influence on precipitation due to the scale of fronts (Kodama et al., 2019).

2.3 ETC hazard footprints

The ETC hazard variables examined are the maximum daily total precipitation (or equivalently the wettest winter day due to an ETC, akin to the Rx1day metric), the maximum 3 second 10m wind gust, and the maximum height of wind waves and wave swell. The first measure relates to the likelihood of flooding, particularly pluvial flooding in urban areas; the second relates to the likelihood of wind damage; and the third relates to the likelihood of coastal flooding from wave overtopping. The hazard footprints resulting from the tracking (Section 2.1) are post-processed to extract the maximum value at each gridpoint the ETC intersects over its lifecycle, or in the case of precipitation the maximum daily accumulation. The choice of analysing the most extreme hazards within the season provides an upper limit on the most hazardous conditions that might be expected based on a relationship with the seasonal modes of variability; this extends previous work that has taken a seasonally aggregate view (e.g., Degenhardt et al., 2022) and may be useful to stress test the resilience of infrastructure and buildings to extreme hazards. An example of the hazard footprints identified from this method for Storm Ciara in February 2020 is shown in Figure 1.

For each winter season, the hazard footprints from all tracked ETCs are overlaid and the maximum value at each gridpoint is then selected for the winter. The resulting field therefore represents the most extreme ETC hazard (maximum 3 second 10m wind gust, maximum hourly wave swell, or daily total precipitation) experienced at each gridpoint in a given winter; these are used in the regression analysis. This approach is distinct from the seasonal average or cumulative perspective that has been used in some other studies and emphasises short-term extreme hazards. Note, the extremes are therefore not spatially contiguous and the values at neighbouring gridpoints may come from different ETCs within a given season.

For part of the analysis, we also calculate a storm damage index (SDI) (Karremann et al. 2014), which is the population weighted meteorological storm severity index (SSI) (Klawns and Ulbrich 2003). The SSI is calculated as

$$SSI_{i,j} = \left(\frac{v_{i,j}^{max}}{v_{i,j}^{98}} - 1 \right)^3, \quad (\text{Equation 1})$$



where i and j are the gridbox coordinates, v_{\max} is the maximum wind speed value associated with the ETC, v_{98} is the 98th percentile of the winter wind speed distribution over 1980-2020. Negative values of SSI are set to zero to ensure cyclonic wind speeds below the 98th percentile threshold do not contribute to the loss metrics.

130 Since the losses associated with windstorms will be strongly related to the exposure of people and buildings, the SSI can be scaled by the population estimate at each grid box to estimate a storm damage index (SDI)

$$SDI_{i,j} = SSI_{i,j} \times population_{i,j}, \quad (\text{Equation 2})$$

where gridded population data for 2015 are taken from the Gridded Population of the World fourth version (GPWv4; doi:10.7927/H49C6VHW). For comparison with earlier studies, the SDI is summed over all storms within a given season to
135 give a seasonal SDI value (e.g., Degenhardt et al., 2022).

2.3 North Atlantic modes of variability

The North Atlantic Oscillation (NAO) and East Atlantic (EA) modes of variability are calculated as the first two empirical
140 orthogonal functions (EOF1 and EOF2) of winter (DJF) mean sea level pressure in the North Atlantic sector (90°W-40°E, 20-80°N) and the associated principal component timeseries (PC1 and PC2). These are hereafter referred to as PC1 and PC2, respectively.

2.4 Regression analysis

145 We perform least squares linear and multiple linear regression of the winter maximum ETC hazards at each gridpoint against the winter mean PC1 and PC2 timeseries within the Euro-Atlantic domain 25°W-40°E, 35-75°N. To assess the suitability of the statistical model to describe the data, we examine the R^2 , linearity, metric homoscedasticity, normality of residuals and the independence using the Durbin Watson (DW) statistic to test for autocorrelation in the residuals. The DW statistic ranges from
150 0 to 4, with a value of 2 indicating zero autocorrelation in the residuals. For linearity, homoscedasticity and normality we assess p-values using a 95% confidence level, such that $p < 0.05$ denotes the required condition is not met and the regression model performance is unsatisfactory, while $p > 0.05$ denotes the condition is met.

Some previous studies have investigated the signals of North Atlantic modes of variability in European SDI and ETC frequency
155 based measures (e.g., Degenhardt et al., 2022). We also tested these metrics but found issues with the performance of linear regression at the grid point scale.

By construction, $SDI = 0$ when $v_{\max} < v_{98}$ (see Equation 1). This non-linear behaviour means a linear regression is likely to perform poorly if applied over all time points. Typical performance of linear regression for SDI against PC1 and PC2 is shown



160 in Figure 2 for a gridpoint near Birmingham (52.5°N, 2.0°E). Figure S1 shows the full statistical metrics for the linear
regression performance for SDI across our study region. While statistically significant regression coefficients against PC1 and
PC2 are obtained in some regions (Figure S1a, cf. Degenhardt et al., 2022), the analysis of the regression performance reveals
the homoskedasticity and normality criteria are poorly met within those regions (Figure S1c), meaning there is too much
variance and non-normal behaviour in the error term and the model isn't well defined. Therefore, while reasonable total R^2
165 values can in principle be achieved (Figure S1b), the linear model is not suitable for this data. Hence, we do not perform further
analysis of SDI in this study. Previous studies have generally presented R^2 values for similar regression analyses but not further
measures of model performance.

ETC frequency related measures, such as total count or number of ETCs exceeding a specified wind gust threshold, are discrete
170 variables where linear regression can perform poorly. Fewer issues were found with the performance of linear regression for
seasonal ETC count (Figure S2), though some European regions show residuals that do not satisfy the criteria of normality or
zero autocorrelation in the residuals. Therefore, we encourage caution in applying simple statistical analyses like linear
regression to data which may not satisfy the requirements for a linear model. For these reasons we do not include frequency
and SDI based ETC hazard metrics in this study.

175

3. Results

3.1 Signatures of NAO and EAP in ETC hazards

180 Figure 3 shows the climatological winter maxima derived from the cyclone footprints and PC1 and PC2 regression maps for
the three ETC hazard types: (a) winter maximum daily precipitation accumulation, (b) winter maximum 10m wind gust and
(c) winter maximum wave swell height. The PC1 and PC2 regression slopes are shown as percentage anomalies from the
climatology, with equivalent absolute anomalies shown in Figure S3. The accompanying R^2 values for the regressions are
shown in Figure 4 and the evaluation of the regression performance is shown in Figure S4, which shows the linear regression
185 performs much better for these variables than those discussed in Section 3.1.

Although there is a well known relationship between PC1 and winter total precipitation in Europe (e.g., McKenna and
Maycock, 2022), there is a relatively weak relationship of PC1 with the winter maximum daily total precipitation from ETCs,
though where a significant relationship is seen the canonical NAO north/south Europe wet/dry dipole pattern is evident. In
190 contrast, a positive PC2 anomaly corresponds with a significant increase in winter maximum daily total precipitation over
Portugal and parts of western UK. Scaife et al. (2008) showed a relationship between 5-day precipitation extremes and the
NAO, with more events above the 90th percentile and less events below the 10th percentile over the UK and northern Europe



during NAO positive. The lack of significant relationship with PC1 could be a result of the relatively noisy data, since at each gridpoint we are taking the wettest day in the winter associated with any ETC and regressing this against the seasonal NAO.

195

In contrast, there is a strong signal of winter maximum 10m wind gust in both PC1 and PC2, with large regions with anomalies of 10-15% above climatology. For positive PC1, the UK, Scandinavia, Netherlands and Northern Germany show increased maximum wind gusts, while Portugal and Northern Spain show a decrease. For positive PC2, southern and south-west England and Wales show an increase wind gust along with Portugal and Spain, while parts of Scandinavia and eastern Mediterranean show a reduction.

200

The patterns of anomalous wave swell height largely mirror those of wind gusts, reflecting their known relationship (e.g., Dobrynin et al., 2019), with positive height anomalies of 10-15% around the UK and Scandinavian coasts for PC1. For PC2, there are comparable anomalies around Southern Ireland and south-west England, as well as anomalies of 5-10% around the French, Portuguese and Spanish coastlines.

205

In regions where the regression coefficients are statistically significant, the combined PC1 and PC2 regressions explain up to around 50% of the interannual variance of the maximum winter wind gust and wave swell height, but less for maximum daily total precipitation over land areas (Figure 4).

210

3.2 Compound multivariate hazards for PC1/PC2

Compound events where multiple hazards coincide in space and time are often particularly impactful (e.g., Owen et al., 2021). Here we consider the overlap of the shaded areas for each hazard in Fig 3 separately for PC1 and PC2 to determine the relative exposure to multiple ETC hazards at a given location. This is shown in Figure 5. Note given these are statistical relationships, we are not establishing whether the extremes occur from the same ETC and are therefore coincident in time; rather, this reflects whether regions could experience enhanced exposure to multivariate hazards within a winter, depending on the relative phases of PC1 and PC2.

215

220

PC1 has a larger influence over land through at least one hazard type than PC2, with the entire UK, northern Germany, the Netherlands, southern Scandinavia and parts of eastern Europe and Russia all having increased exposure to at least one hazard type (Figure 5). This largely reflects the more extensive PC1 signal in maximum wind gust in these regions. The areas exposed to two hazard types are mainly limited to marine and coastal regions surrounding the UK and Norwegian and Baltic Seas, reflecting the intersection of wind gust and wave swell hazards. Almost no areas show increased exposure to all three hazards for PC1.

225



For PC2, there is no discernible increase in exposure to any single hazard across France, Germany, most of Scandinavia, eastern Europe, Scotland, Northern Ireland and Northern England (Fig. 5b). Land and coastal areas in Wales, Southern England, Spain and Portugal all show increased exposure to at least two hazards, which over land areas reflects elevated wind gust and maximum daily precipitation and over ocean elevated wind gust and wave swell. The coasts around southern Ireland, Wales, southern England, northern France and Portugal show intersection of increased in all three hazards (i.e. wetter, windier and higher wave swell) under positive PC2.

3.3 Compound hazards for combined PC1/PC2 circulation

Given that many winters show anomalous North Atlantic atmospheric circulation that partly projects onto both PC1 and PC2, we next consider the overlap between the PC1 and PC2 patterns for each variable separately, to identify where the two modes have joint signals that would influence the risk of exposure to ETC hazards (Figure 6). This reveals virtually no regions of compound maximum daily precipitation hazards over land, but coherent regions where PC1 and PC2 affect variability for wind gusts and wave swell. These regions are Portugal, southern England, Wales, southern Ireland, southern Scandinavia. As before, over ocean points the patterns for the two variables are similar given that wave swell is strongly driven by near-surface wind. The overlapping patterns for these variables indicates the absolute change in exposure to ETC hazards in a given winter will be affected by the relative amplitudes of PC1 and PC2.

To further illustrate this, Figure 7 shows absolute values of the expected ETC hazards for unitary combinations of the standardised PC1 and PC2 indices (i.e. +1 PC1 and +1 PC2; +1 PC1 and -1 PC2, etc). These are constructed by superposing the PC1 and PC2 signals onto the winter climatology over all years. The scatterplot in the centre of Figure 7 shows the combinations of PC1/PC2 indices in ERA5 for all winters from 1980-2022. Some combinations have been observed infrequently (PC1<0 and PC2<0), which shows it is rarely the case that negative NAO occurs with Atlantic ridging, but all four combinations of indices used to present the hazards lie within the distribution of observed PC1/PC2 indices and are therefore plausible examples. The hazard maps include solid contours denoting specific thresholds for wind gusts, based on the Beaufort scale for severe gale (25 m/s), violent storm (29 m/s) and hurricane strength (33 m/s) gusts, and for wave swell height based on the Douglas Sea Scale, for very high (9m) and phenomenal (14m) heights.

For the combination PC1– and PC2+, the winter maximum wind gust reaches violent storm intensity along the west coast of Ireland and the Bay of Biscay and severe gale intensity along the Iberian peninsula and Norwegian coast. The maximum wave swell reaches very high along the west coast of Ireland and precipitation is 10-30% above normal in southern Ireland, England and Iberia, with drier conditions in Scandinavia.



260 In comparison, for the combination of PC1+ and PC2+ the winter maximum wind gust reaches hurricane intensity along the west coast Ireland, in Wales, south-west England and Scotland, with severe gale intensity in south-east England. Maximum wind gust reaches violent storm intensity along the Norway, Sweden and Finland coastlines. The area where winter maximum wave swell reaches very high levels is expanded compared to PC1- and PC2+, reaching south-west England and extending into the Norwegian Sea. Precipitation is 10-30% above normal in northern Scotland and the Iberian peninsula.

265

For PC1+ combined with PC2-, the area where winter maximum wind gust reaches hurricane intensity extends further east towards the Norwegian coast, with violent storm intensity near south-west England and Wales. In contrast, in southern Europe winter maximum wind gust is alleviated reaching less than severe gale force in the Iberian peninsula and severe gale force in the Bay of Biscay, Sweden and southern Finland. The region exposed to very high maximum wave swell height reaches the west of Ireland, Scotland, southern Iceland and the northern Norway coast. Precipitation shows drier than normal conditions in southern Ireland, England and Iberia, with above average precipitation in Scandinavia.

270

Lastly for PC1- combined with PC2-, winter maximum wind gust reaches severe gale intensity in the Bay of Biscay, with below severe gale level in southern England and Wales. Along the west coast of Ireland, northern Scotland and the Norwegian coast the maximum wind gust reaches violent storm intensity. The region exposed to very high wave swell is more restricted to the west of Ireland. Maximum daily total precipitation is 10-30% below normal in northern Scotland and Iberia.

275

These examples illustrate the importance of the signals of extreme ETC hazards associated with PC1 and PC2 variability for the exposure of different parts of Europe to the risk of severe weather events.

280

4. Discussion and conclusions

This study has investigated the relationships between extreme meteorological hazards in Europe associated with ETCs and the two leading modes of North Atlantic atmospheric variability: the North Atlantic Oscillation (PC1) and the East Atlantic pattern (PC2). ETCs were tracked and their footprints in key hazard variables - winter maximum 10m wind gust, maximum wave swell height and maximum daily total precipitation - were extracted. The relationship of these variables with the seasonal winter NAO and EAP indices were derived using linear regression. In contrast to earlier work, we focus on the most extreme event for a particular variable and location within a winter season and the year-to-year relationship of those extremes with large-scale modes of variability. The motivation for this is to understand the nature of the most extreme hazard that can be expected to occur in a typical winter characterised by NAO and EAP circulation anomalies.

290

There are significant relationships of PC1 and PC2 with the ETC hazard variables in many regions of Europe. These overlap in some regions, indicating an interaction between modes of variability for the exposure in those regions to risks from weather



300 hazards. We have further considered compound events where there may be increased exposure to multiple ETC hazards within
295 a season. This was particularly the case for wind gust and wave swell height, which are physically coupled.

We have also shown that some common ETC and hazard indices are not well suited to the application of linear regression at
the grid point level, notably the storm damage index (SDI) and discrete variables like storm frequency, meaning other studies
should carefully consider the suitability of their methods.

300

The findings of the study highlight the potential for predictive skill of large-scale modes on seasonal timescales (e.g., Scaife
et al., 2014; Thornton et al., 2023) to be used to quantify the expected exposure to extreme winter ETC hazards in Europe.
Since these events are regularly responsible for billions of euros of damages, this could provide information for stakeholders
in the insurance, transport, energy and housing sectors.

305

References

Bacon, S. and Carter, D.J.T. (1993), A connection between mean wave height and atmospheric pressure gradient in the North
Atlantic. *Int. J. Climatol.*, 13: 423-436. <https://doi.org/10.1002/joc.3370130406>

310

Bandhauer, M., Isotta, F., Lakatos, M., Lussana, C., Båserud, L., Izsák, B., Szentes, O., Tveito, O. E.,
& Frei, C. (2022). Evaluation of daily precipitation analyses in E-OBS (v19.0e) and ERA5 by comparison to regional high-
resolution datasets in European regions. *International Journal of Climatology*, 42(2), 727–
747. <https://doi.org/10.1002/joc.7269>

315

Befort DJ, Wild S, Knight JR, *et al.* Seasonal forecast skill for extratropical cyclones and windstorms. *Q J R Meteorol
Soc.* 2019; 145: 92–104. <https://doi.org/10.1002/qj.3406>

Bloomfield H, Hillier J, Griffin A, Kay A, Shaffrey L, Pianosi F, James R, Kumar D, Champion A and Bates P 2023 Co-
320 occurring wintertime flooding and extreme wind over Europe, from daily to seasonal timescales *Weather Clim.
Extremes* **39** 100550

Castelle, B., Dodet, G., Masselink, G., & Scott, T. (2018). Increased winter-mean wave height, variability, and periodicity in
the northeast Atlantic over 1949–2017. *Geophysical Research Letters*, 45, 3586–
325 3596. <https://doi.org/10.1002/2017GL076884>



Center for International Earth Science Information Network (CIESIN), Columbia University. 'Gridded Population of the World, Version 4 (GPWv4): Population Density, Revision 11.' Palisades, NY: Socioeconomic Data and Applications Center (SEDAC), 2017. doi:10.7927/H49C6VHW

330

Degenhardt, L., Leckebusch, G.C. & Scaife, A.A. Large-scale circulation patterns and their influence on European winter windstorm predictions. *Clim Dyn* **60**, 3597–3611 (2023). <https://doi.org/10.1007/s00382-022-06455-2>

Degenhardt, L., Leckebusch, G. C., and Scaife, A. A.: Understanding winter windstorm predictability over Europe, *Weather Clim. Dynam.*, 5, 587–607, <https://doi.org/10.5194/wcd-5-587-2024>, 2024.

335

Dobrynin, M., Kleine, T., Düsterhus, A., & Baehr, J. (2019). Skilful seasonal prediction of ocean surface waves in the Atlantic Ocean. *Geophysical Research Letters*, 46, 1731–1739. <https://doi.org/10.1029/2018GL081334>

340 Dodet, G., X. Bertin, and R. Taborda, Wave climate variability in the North-East Atlantic over the last six decades, *Ocean Model.* **31**, 120–131 (2010).

Donat, M.G., Leckebusch, G.C., Pinto, J.G. and Ulbrich, U. (2010), Examination of wind storms over Central Europe with respect to circulation weather types and NAO phases. *Int. J. Climatol.*, 30: 1289-1300. <https://doi.org/10.1002/joc.1982>

345 European Center for Medium-Range Weather Forecasts (ECMWF) (2016) IFS Documentation CY45R2—Part IV: Physical processes. IFS doc. <https://www.ecmwf.int/node/16648>. Accessed 8 May 2020

Hersbach H, Bell B, Berrisford P, et al. The ERA5 global reanalysis. *Q J R Meteorol Soc.* 2020; 146: 1999–2049. <https://doi.org/10.1002/qj.3803>

350

Hillier J K, Macdonald N, Leckebusch G C and Stavrinos A 2015 Interactions between apparently primary weather-driven hazards and their cost *Environ. Res. Lett.* **10** 104003

355 Hillier, J.K., Bloomfield, H.C., Manning, C., Garry, F., Shaffrey, L., Bates, P. and Kumar, D. (2025), Increasingly Seasonal Jet Stream Raises Risk of Co-Occurring Flooding and Extreme Wind in Great Britain. *Int J Climatol* e8763. <https://doi.org/10.1002/joc.8763>

Hodges, K. I.: A General Method for Tracking Analysis and Its Application to Meteorological Data, *Mon. Weather Rev.*, 122, 2573–2586, [https://doi.org/10.1175/1520-0493\(1994\)122<2573:AGMFTA>2.0.CO;2](https://doi.org/10.1175/1520-0493(1994)122<2573:AGMFTA>2.0.CO;2), 1994.



360

Hodges, K. I.: Feature Tracking on the Unit Sphere, *Mon. Weather Rev.*, 123, 3458–3465, [https://doi.org/10.1175/1520-0493\(1995\)123<3458:FTOTUS>2.0.CO;2](https://doi.org/10.1175/1520-0493(1995)123<3458:FTOTUS>2.0.CO;2), 1995.

Hodges, K. I.: Adaptive Constraints for Feature Tracking, *Mon. Weather Rev.*, 127, 1362–1373, [https://doi.org/10.1175/1520-0493\(1999\)127<1362:ACFFT>2.0.CO;2](https://doi.org/10.1175/1520-0493(1999)127<1362:ACFFT>2.0.CO;2), 1999.

Hurrell, J.W., Kushnir, Y., Ottersen, G. and Visbeck, M. (2003). An Overview of the North Atlantic Oscillation. In *The North Atlantic Oscillation: Climatic Significance and Environmental Impact* (eds J.W. Hurrell, Y. Kushnir, G. Ottersen and M. Visbeck). <https://doi.org/10.1029/134GM01>

370

Izaguirre, C., F. J. Mendez, M. Menendez, A. Luceño, and I. J. Losada (2010), Extreme wave climate variability in southern Europe using satellite data, *J. Geophys. Res.*, 115, C04009, doi:[10.1029/2009JC005802](https://doi.org/10.1029/2009JC005802).

Izaguirre, C., F. J. Méndez, M. Menéndez, and I. J. Losada (2011), Global extreme wave height variability based on satellite data, *Geophys. Res. Lett.*, 38, L10607, doi:[10.1029/2011GL047302](https://doi.org/10.1029/2011GL047302).

Karremann, M. K., Pinto, J. G., von Bomhard, P. J., and Klawa, M.: On the clustering of winter storm loss events over Germany, *Nat. Hazards Earth Syst. Sci.*, 14, 2041–2052, <https://doi.org/10.5194/nhess-14-2041-2014>, 2014.

Klawa, M. and Ulbrich, U.: A model for the estimation of storm losses and the identification of severe winter storms in Germany, *Nat. Hazards Earth Syst. Sci.*, 3, 725–732, <https://doi.org/10.5194/nhess-3-725-2003>, 2003.

Kodama, C., Stevens, B., Mauritsen, T., Seiki, T., & Satoh, M. (2019). A New Perspective for Future Precipitation Change from Intense Extratropical Cyclones. *Geophysical Research Letters*, 46, 12435–12444. <https://doi.org/10.1029/2019GL084001>

Lockwood, J. F., N. Dunstone, L. Hermanson, G. R. Saville, A. A. Scaife, D. Smith, and H. E. Thornton, 2023: A Decadal Climate Service for Insurance: Skillful Multiyear Predictions of North Atlantic Hurricane Activity and U.S. Hurricane Damage. *J. Appl. Meteor. Climatol.*, 62, 1151–1163, <https://doi.org/10.1175/JAMC-D-22-0147.1>.

390

Lodise, J.; Merrifield, S.; Collins, C.; Behrens, J.; Terrill, E. Performance of ERA5 wind speed and significant wave height within Extratropical cyclones using collocated satellite radar altimeter measurements. *Coast. Eng. J.* **2024**, 66, 89–114.



395 Martínez-Asensio, A., Tsimplis, M.N., Marcos, M., Feng, X., Gomis, D., Jordà, G. and Josey, S.A. (2016), Response of the
North Atlantic wave climate to atmospheric modes of variability. *Int. J. Climatol.*, 36: 1210-
1225. <https://doi.org/10.1002/joc.4415>

400 Martius, O., S. Pfahl, and C. Chevalier (2016), A global quantification of compound precipitation and wind
extremes, *Geophys. Res. Lett.*, 43, 7709–7717, doi:[10.1002/2016GL070017](https://doi.org/10.1002/2016GL070017).

Matthews, T., Murphy, C., Wilby, R. *et al.* Stormiest winter on record for Ireland and UK. *Nature Clim Change* 4, 738–740
(2014). <https://doi.org/10.1038/nclimate2336>

405 Minola, L., Zhang, F., Azorin-Molina, C. *et al.* Near-surface mean and gust wind speeds in ERA5 across Sweden: towards an
improved gust parametrization. *Clim Dyn* 55, 887–907 (2020). <https://doi.org/10.1007/s00382-020-05302-6>

Moemken, J., Alifdini, I., Ramos, A. M., Georgiadis, A., Brocklehurst, A., Braun, L., and Pinto, J. G.: Insurance loss model
vs. meteorological loss index – how comparable are their loss estimates for European windstorms?, *Nat. Hazards Earth Syst.*
Sci., 24, 3445–3460, <https://doi.org/10.5194/nhess-24-3445-2024>, 2024.

410 Owen LE, Catto JL, Stephenson DB, Dunst one NJ. Compound precipitation and wind extremes over Europe and their
relationship to extratropical cyclones. *Weather Clim Extremes* (2021) 33:100342. doi: 10.1016/j.wace.2021.100342

Priestley, M. D. K., & Catto, J. L. (2022). Improved representation of extratropical cyclone structure in HighResMIP models.
415 *Geophysical Research Letters*, 49, e2021GL096708. <https://doi.org/10.1029/2021GL096708>

Scaife, A. A., C. K. Folland, L. V. Alexander, A. Moberg, and J. R. Knight, 2008: European Climate Extremes and the North
Atlantic Oscillation. *J. Climate*, 21, 72–83, <https://doi.org/10.1175/2007JCLI1631.1>.

420 Scaife, A. A., et al. (2014), Skillful long-range prediction of European and North American winters, *Geophys. Res.*
Lett., 41, 2514–2519, doi:[10.1002/2014GL059637](https://doi.org/10.1002/2014GL059637).

425 Thornton, H. E., Smith, D. M., Scaife, A. A., & Dunstone, N. J. (2023). Seasonal predictability of the East Atlantic Pattern in
late autumn and early winter. *Geophysical Research Letters*, 50, e2022GL100712. <https://doi.org/10.1029/2022GL100712>

Acknowledgements



ACM, CMM and JP acknowledge funding from the H2020 CONSTRAIN project (grant agreement no. 820829). ACM
acknowledges funding from the NERC Stratelust project (NE/X011933/1). JP was funded by the EPSRC Centre for Doctoral
430 Training in Fluid Dynamics at Leeds (EP/S022732/1).

Author contributions

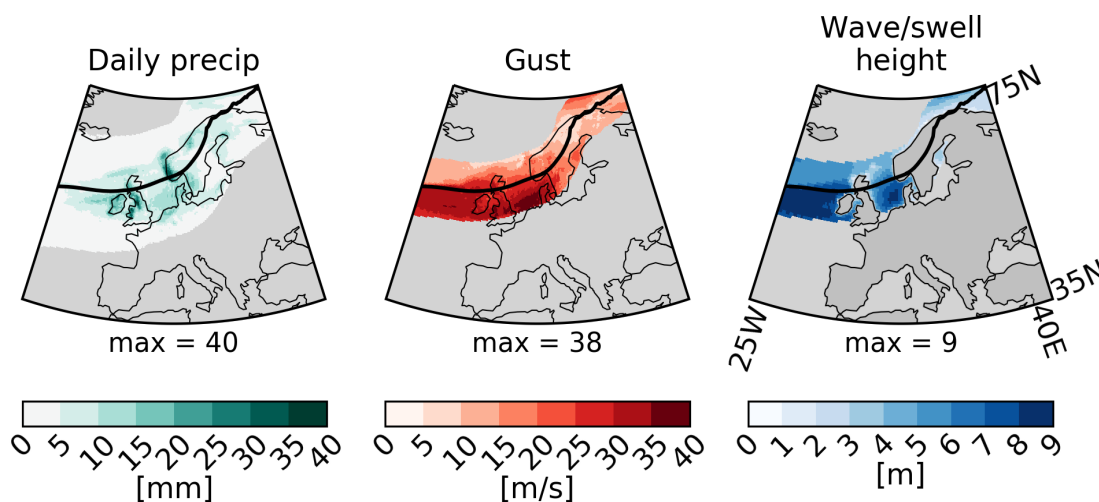
ACM conceived the study. MDKP produced the storm tracks and cyclone footprints. CMM analysed the data and produced
435 figures. JP produced figures. ACM wrote the paper with contributions from all authors.

Data availability statement

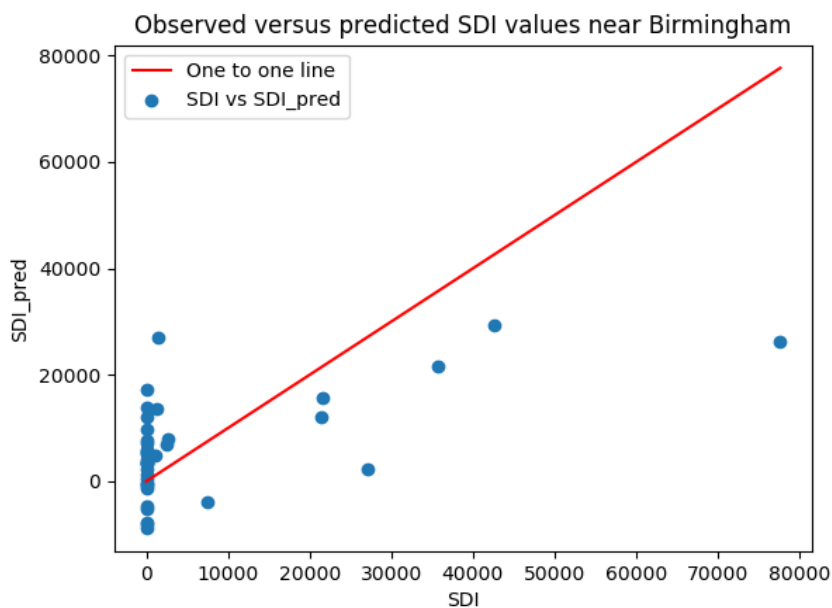
The ERA5 data is available for the Copernicus Climate Data Store. The TRACK algorithm is available on request from Kevin
440 Hodges at the University of Reading.



Max footprints for Storm Ciara, February 2020



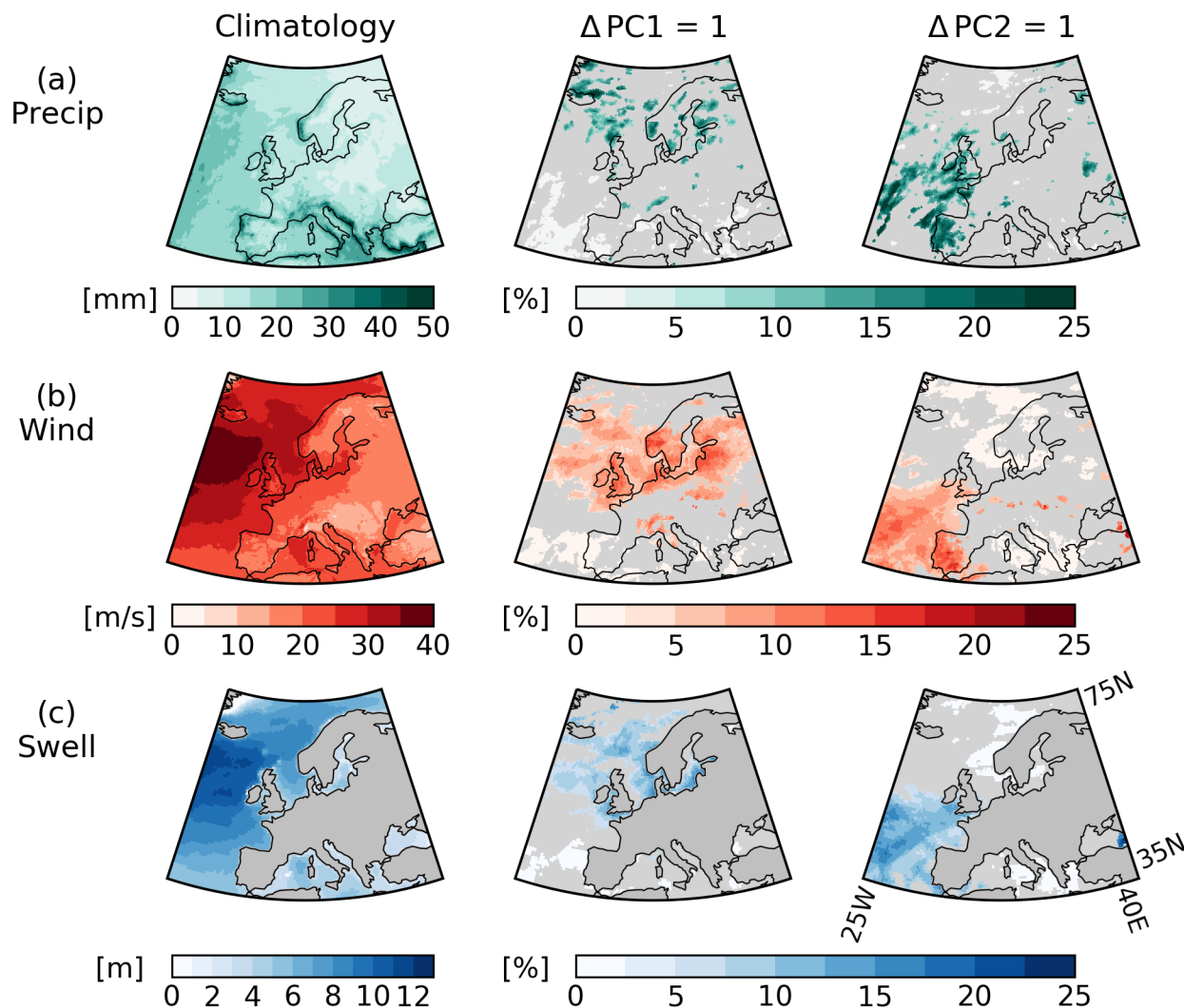
445 **Figure 1:** An example ETC footprint lifecycle for the three measures of ETC hazards (a) local maximum daily total precipitation over lifetime, (b) local maximum 10m wind gust over lifetime, and (c) local maximum wave swell height over lifetime for Storm Ciara in February 2020 (track shown by black line).



450 **Figure 2:** Winter cumulative SDI (x-axis) vs. predicted SDI based on the multiple linear regression between SDI and the PC1 and PC2 timeseries (y-axis) at grid box (1.875°W, 52.5°N). Red line shows 1:1 line. Note some of the predicted SDI values are negative when it is bounded at 0.



Maximum for all cyclones in a winter, ERA5 1981-2020



455

Figure 3: Maximum winter ETC hazards for (a) daily total precipitation [mm], (b) 10m wind gust [m/s] and (c) maximum wave swell height [m] for (left column) climatology, (middle column) regression onto PC1 and (right column) regression onto PC2 shown as percentage anomalies from the climatology. Note wave swell height is only defined over ocean points. Grey areas in middle and right columns denote regions where the regression slope is not significantly different from zero at the 95% confidence level.

460

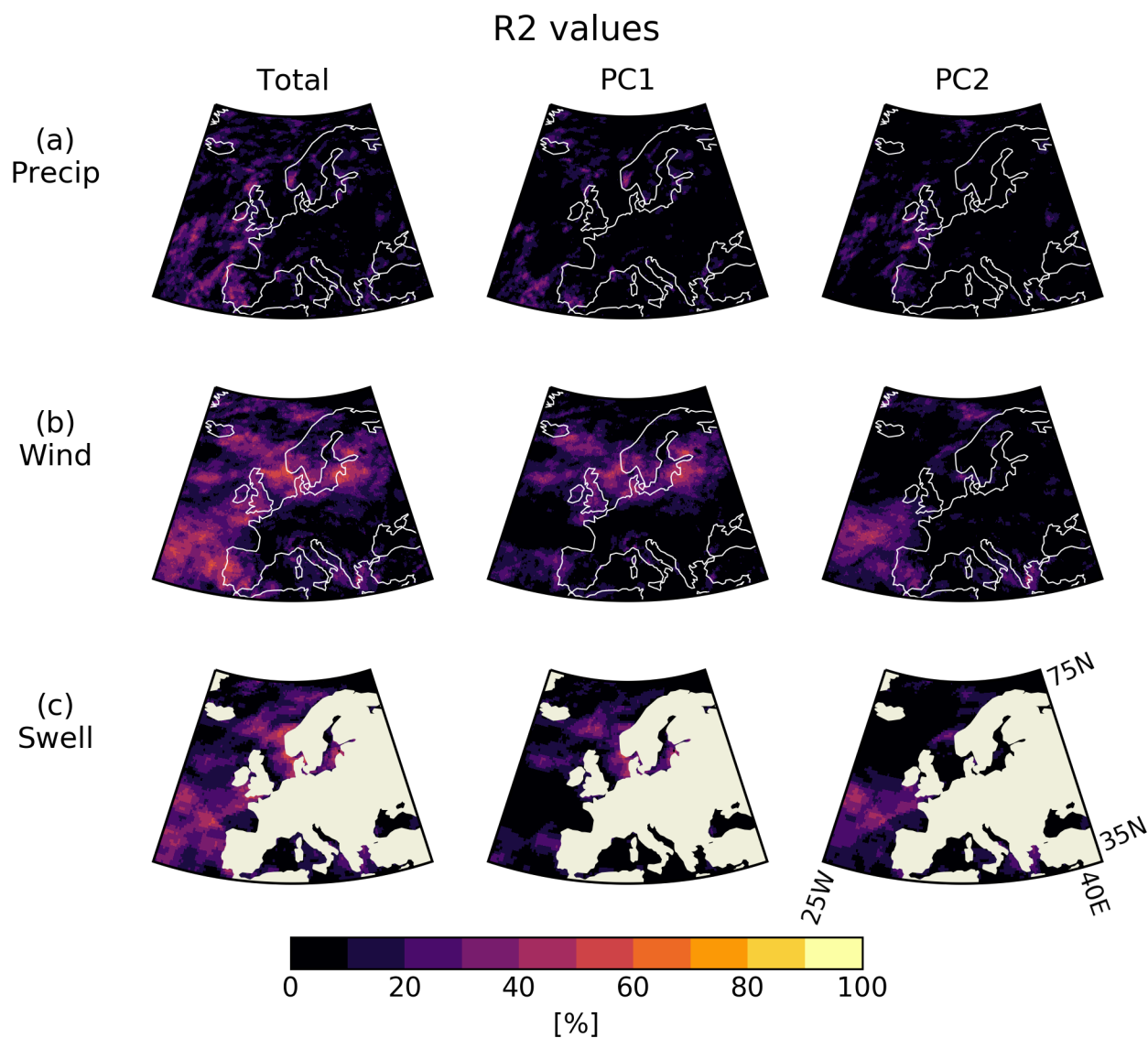


Figure 4: R² values [%] for the linear regression of ETC winter hazards (a) maximum daily total precipitation, (b) maximum 10m wind gust and (c) maximum wave swell height for (left) PC1+PC2, (middle) PC1 and (right) PC2.



Compound impact locations for PC1 and PC2 when considering max for all cyclones in a season, ERA5 DJF 1981-2010

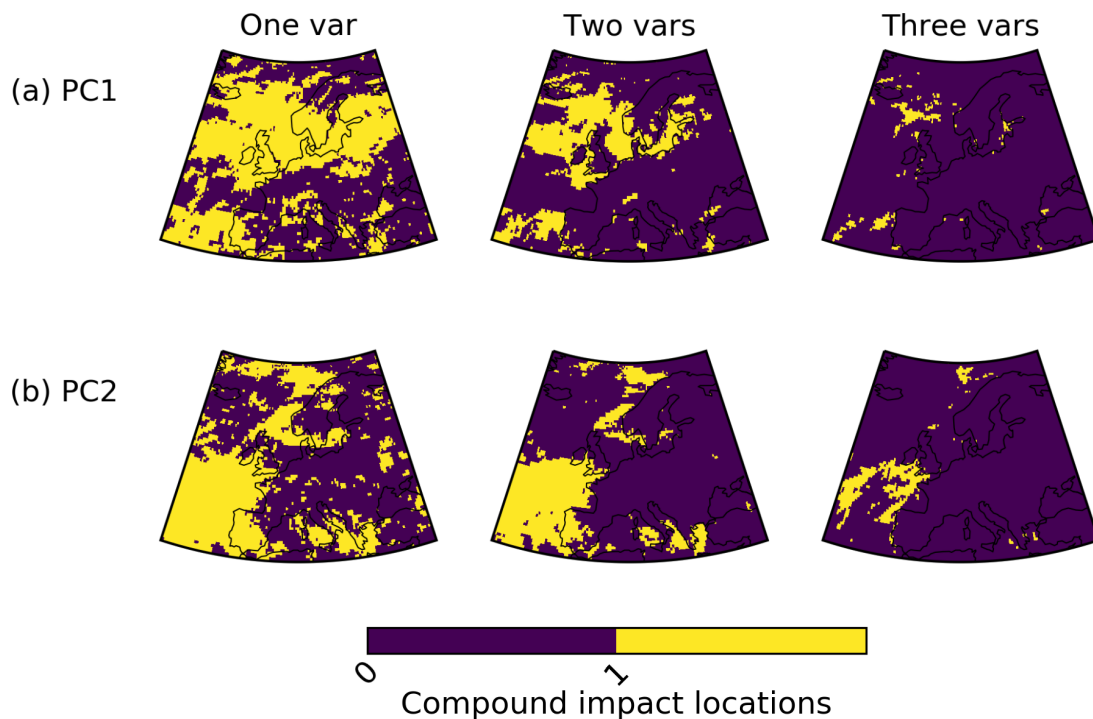


Figure 5: Coincident multivariate spatial signals in ETC hazards for (a) PC1 and (b) PC2. Yellow denotes (Left) all regions affected by at least one hazard type; (middle) regions affected by at least two hazard types; (right) regions affected by all three hazard types. Purple denotes no effect (left) or no compound effect (middle/right).



Compound impact locations for PC1+PC2 when considering max for all cyclones in a season, ERA5 DJF 1981-2010

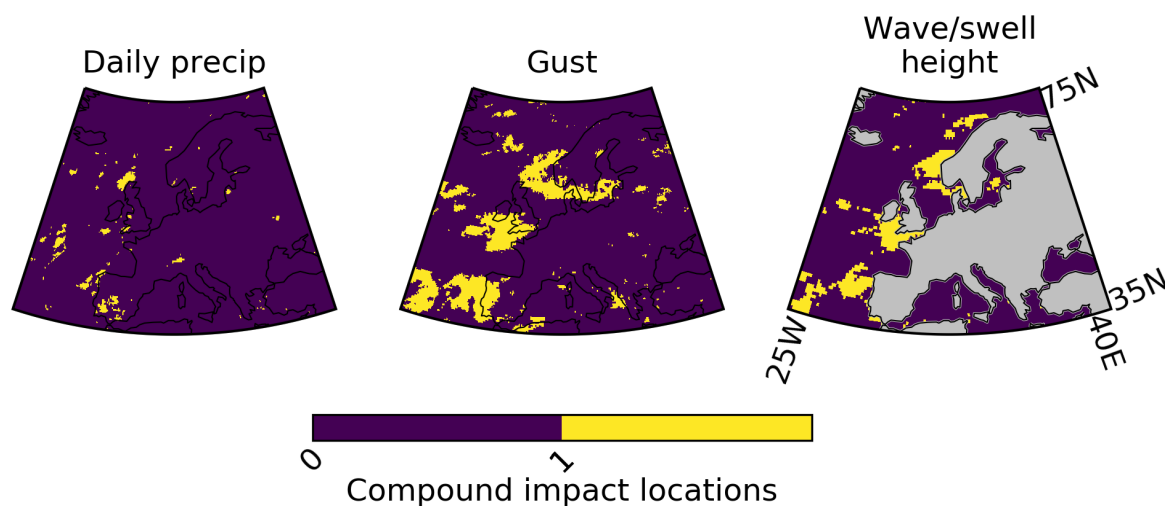
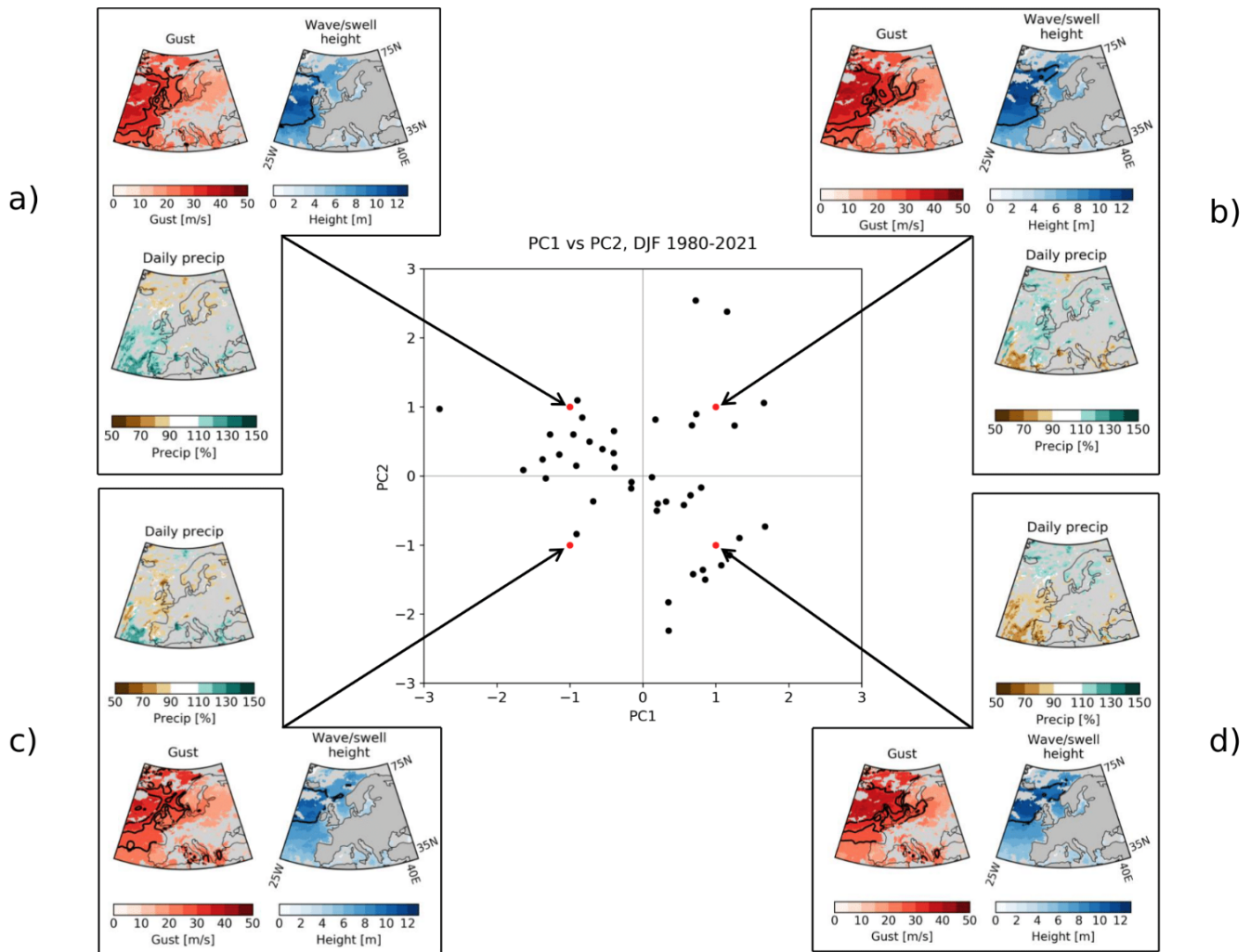


Figure 6: Coincident spatial signals for combined PC1 and PC2 in individual ETC hazards (a) winter maximum daily total precipitation, (b) winter maximum 10m wind gust and (c) winter maximum wave swell height. Yellow denotes compound impact locations between PC1 and PC2 for each hazard, purple denotes no effect or no compound effect.

475



480

Figure 7: Absolute values of winter maximum 10m wind gust (m/s) and maximum wave swell height (m), with maximum daily total precipitation shown as a percentage of climatology (%) predicted by the linear regression model for unitary combinations of positive and negative PC1/PC2 indices (red dots in middle panel). Black contours in gust panels show 25 m/s (severe gale), 29 m/s (violent storm), 33 m/s (hurricane strength) thresholds based on the Beaufort scale. Black contours in wave swell height panels show 9 m (very high) and 14 m (phenomenal) based on the Douglas Sea Scale. Black points in middle panel show historical winter PC1/PC2 indices from ERA5.

485